Regenerative Therapy 14 (2020) 48–58

Contents lists available at ScienceDirect

Regenerative Therapy

journal homepage: http://www.elsevier.com/locate/reth

Original Article

Recovery of sensory function after the implantation of oriented-collagen tube into the resected rat sciatic nerve

Keita Otake [a], Taku Toriumi [b], Tatsuaki Ito [a], Yuta Okuwa [b], Keiichi Moriguchi [b], Sho Tanaka [a], Yoshihiro Isobe [c], Taro Saku [c], Kenichi Kurita [a], Masaki Honda [b, *]

[a] Department of Oral and Maxillofacial Surgery, School of Dentistry, Aichi Gakuin University, 2-11 Suemori-dori, Chikusa-ku, Nagoya, Aichi, 464-8651, Japan
[b] Department of Oral Anatomy, School of Dentistry, Aichi Gakuin University, 1-100 Kusumoto-cho, Chikusa-ku, Nagoya, Aichi, 464-8650, Japan
[c] Atree. Inc., 16-12-1 Hiroo, Shibuya-ku, Tokyo, 150-0012, Japan

ARTICLE INFO

Article history:
Received 11 November 2019
Received in revised form
3 December 2019
Accepted 5 December 2019

Keywords:
Biocompatible materials
Peripheral nerves
Nerve regeneration
Sciatic nerve
Microscopy

ABSTRACT

Introduction: In the present study, we examined the effect of oriented collagen tube (OCT) implantation on the recovery of sensory function of the resected rat sciatic nerve.
Materials and methods: After a 10-mm long portion of the sciatic nerve of a rat was resected, an OCT was placed in the site of nerve defect. Recovery of the sensory function was evaluated using Von Frey test every 3 days after surgery. The regenerated tissue were histologically and ultrastructurally analyzed 2 and 4 weeks after the surgery.
Results: The sensory reflexes of the OCT group were restored to the level of that of the intact group after 15 days. Hematoxylin and eosin staining revealed the cross-linking between the proximal and distal stumps after 2 weeks. After 4 weeks, Luxol Fast Blue and immunohistochemical staining revealed the presence of myelin sheath from the proximal to distal region of the regenerated tissue and S100B staining confirmed the presence of Schwann cells. Interestingly, no myelin sheath was ultrastructurally observed around the regenerated axons at the central region after 2 weeks.
Conclusions: These results suggest that OCTs facilitate the recovery of sensory function. Additionally, the non-myelinated axons contributed to the recovery of the sensory function.

1. Introduction

Peripheral nerve injury results in functional and morphological changes in the nervous, connective, and muscle tissues innervated by the injured branch. Although endogenous peripheral nerve regeneration is possible, it is often insufficient for complete functional recovery; the extent of recovery is similar to that limited by the size of the nerve gap, neuroma formation, and scar tissue formation [1]. Therefore, it has a devastating major impact on a patient's quality of life. Typical symptoms are sensory and motor function defects that could result in complete paralysis of an affected organ or development of neuropathic pain. In the case of failed recovery, surgical repair techniques including nerve grafting are usually used to treat transectional nerve injuries [2,3].

Repair of peripheral nerve injury is currently an important research topic in the fields of neurosurgery and oral-maxillofacial surgery. The aim of treatment is to promote nerve regeneration, maintain muscle mass, enhance muscle strength, and promote functional recovery. However, several difficulties associated with the repair of peripheral nerve injury have been reported [4,5]. The three main concerns are as follows: 1)the effective and accurate connection of fibers with different characteristics, such as sensory and motor nerves, in both distal and proximal ends of the injury site; 2) provision of sufficient number of nerve fibers by the proximal end to innervate the proximal target organ; and 3) keeping the motor end plates of distal target organ from destabilizing and minimizing muscle atrophy before the regenerating proximal nerve fibers grow into and innervate the target organ [6]. Various

Abbreviations: OCT, oriented collagen tube; PODs, postoperative days; PBS, phosphate buffered saline; H&E, hematoxylin and eosin; LFB, Luxol Fast Blue; MBP, myelin basic protein; TEM, transmission electron microscopy; SD, standard deviation; IAN, inferior alveolar nerve.

* Corresponding author. Fax: +81 52 752 5988.
E-mail address: honda-m@dpc.agu.ac.jp (M. Honda).

Peer review under responsibility of the Japanese Society for Regenerative Medicine.

https://doi.org/10.1016/j.reth.2019.12.004

researchers have concentrated on different peripheral nerve repair procedures to better promote fiber regeneration across the abutment joint, as well as to protect the distal target organs effectively [7,8]. Recently, the use of artificial nerve conduits as nerve graft substitutes has become increasingly common. Poly-glycolic acid, silicone, and collagen have already been used as conduit materials for guiding nerve regeneration in the clinical setting [9]. However, there is still no consensus regarding the most effective approach for the regeneration of a defective peripheral nerve.

A correlation between the orientation of the substrate and the directional growth of cells as contact guidance was proposed by Weiss [10]. Thereafter, the unique ability of aligned collagen to dictate the orientation of cells was discovered and the contact guidance technique was developed to fabricate anisotropic substrates of collagen [11,12]. The correlation of cell orientation with collagen fibril orientation was first reported by using a three-dimensional culture model of fibroblasts in a pre-aligned collagen gel with various levels of orientation [13]. Until now, production of collagen scaffolds of the desired size and orientation for use in the clinical setting has been difficult due to the requirement of complex equipment and involvement of complex processes. An oriented collagen tube (OCT) in a three-dimensional string form was developed by arraying flow-oriented collagen string gels and dehydrating them to overcome these problems [6]. Using this technique, the size of scaffolds and the direction of orientation of strings can be controlled easily. The multilayered OCT has been successfully used as an implant material for blood grafting the carotid artery of rabbits [6]. Furthermore, another study showed that cultured osteoblasts seeded on OCT exhibited preferential alignment along the substrate collagen fiber orientation [14].

The process of peripheral nerve regeneration after injury involves the following major events: Wallerian degeneration, axon regeneration/growth, and nerve reinnervation. The major determinant of functional recovery after injury is the accuracy of axon regeneration to its original target end organs. Schwann cells also play a crucial role in the regeneration of axons by reconstructing myelin [15–19]; regenerating axons exhibit a strong preference to grow along basal lamina tubes reconstructed by Schwann cells [20–22]. Furthermore, a previous study showed that the orientation of Schwann cells influences the axonal outgrowth *in vitro* [23]. To summarize, the environment of a peripheral nerve may have a significant effect on the behavior of Schwann cells during peripheral nerve regeneration. We speculated that the establishment of myelin sheath morphogenesis could be driven by the directional control of Schwann cells, because tissue anisotropy is considered to be closely associated with the shape [24], polarization [25,26], or arrangement [27] of the constituent cells. In a previous study, OCTs were grafted to repair a long gap in the rat sciatic nerve [28]. Examination of the regenerative outcome, including catwalk and electron microscopy analyses, was carried out 4 and 8 weeks after OCT implantation. The myelin sheath was slightly observed after 4 weeks; however, the sensory function was not evaluated after OCT implantation. In the craniomaxillofacial area, the inferior alveolar nerve (IAN) is a part of the mandibular division of the trigeminal nerve as sensory neuron. The IAN can be damaged during the removal of the third molars or as a result of orthognathic surgery or mandibular fractures [29,30]. Therefore, the development of a method for the treatment of an injured sensory neuron as well as the recovery of the motor neuron function is a challenge of great importance. Therefore, the purpose of the present study is to examine the effect of OCT implantation on recovery of the sensory function by using Von Frey test and to perform histological and ultrastructural analyses.

2. Materials and methods

All experimental procedures involving animals were carried out in accordance with the Institutional Animal Care guidelines and approved by the Animal Care and Use Committee for the School of Dentistry, Aichi Gakuin University (Approval number: AGUD379).

2.1. Fabrication of the oriented collagen tubes

OCTs were fabricated as described before [6]. Briefly, pepsin-solubilized porcine skin type-I atelocollagen (Nippi, Tokyo, Japan) at a concentration of 10 mg/mL in 0.02 N acetic acid (pH 3.5) was used for the fabrication of collagen gel strings. Collagen gel strings were prepared using a deposition system consisting of a three-axis robotic arm (SM 300-3 A; Musashi Engineering, Tokyo, Japan) equipped with a syringe. The syringe was equipped with a flexible polypropylene 22-G needle to allow the existing fluid to be ejected parallel to the target surface (Fig. 1A). Moving the fluid and the robot in opposite directions yields an expanded flow component in the discharged fluid. The deposition speed of the robotic arm was set to 550 mm/s, and the air pressure applied to the collagen solution was set to 0.1 MPa. After the injection of collagen gel strings, they were demineralized and aligned on a polypropylene rod seven times to fabricate a seven-layer seamless tube (Fig. 1B). The length and internal diameter of the OCT prepared were 14 mm and 1.5 mm, respectively (Fig. 1C). The orientation of collagen fibers in the seven-layer collagen tube was analyzed by scanning electron microscopy (JXA-8530FA, JEOL Ltd., Tokyo, Japan), and the collagen fibers had a certain orientation with regularly arrangement (Fig. 1D).

2.2. Rat sciatic nerve resection model

The procedure for resecting the rat sciatic nerve was previously described [28]. Briefly, the left sciatic nerve was exposed (Fig. 2A) and a segment was transected to generate a defect that is 10 mm in length ($n = 10$). In the experimental group (OCT group), the 10-mm gap was repaired using 14-mm long OCTs (Fig. 2B). Portions of the distal and proximal nerve stumps (2 mm) were inserted into the OCT and the proximal or distal nerve stumps and OCTs were sutured with 10-0 nylon thread. Thereafter, the muscle layer and epidermis were sutured with 4-0 silk threads to close the wound. In the defect group (defect group), the 10-mm long defect generated in the sciatic nerve was resected but it was not treated with an OCT ($n = 8$). In the sham operation group (sham group), the wound was immediately closed after the exposure of the left sciatic nerve ($n = 8$). The normal control group included uninjured rats with an intact sciatic nerve (intact group) ($n = 8$).

2.3. Von Frey test

Rats ($n = 8$ for the OCT group, defect group, and sham group) were subjected to the Von Frey test on postoperative days (PODs) 3, 6, 9, 12, and 15. To evaluate the mechanical stimulation sensitivity, the 50% withdrawal threshold was determined using the up-down method as described previously [31,32]. Briefly, rats were individually placed on a 5 mm × 5 mm wire-mesh grid floor in a plastic cage. Following acclimation to the test cage for 1 h, calibrated Von Frey filaments (TACTILE TEST AESTHESIO Semmes-Weinstein Von Frey Aesthesiometer, Muromachi Kikai Co., Ltd, Tokyo, Japan) were applied to the middle of the plantar surface of the hind paw at an angle of 90° through the bottom of the mesh floor. In this paradigm, testing was initiated with a 60 g force in the middle of the series (8, 10, 15, 26, 60, 100, 180, and 300 *g*) and held for 3–5 s with the filament slightly buckled. Stimuli were always presented in a

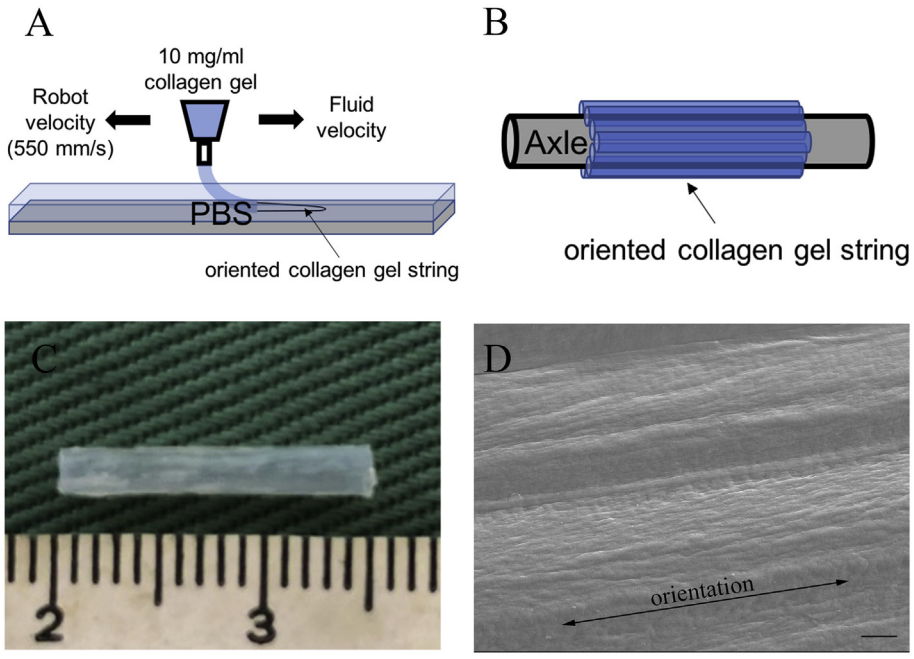

Fig. 1. Preparation of oriented collagen tubes (OCTs). (A) Schematic illustration of the robotic deposition of collagen gel in PBS buffer. (B) After the injection of collagen gel strings, they are demineralized and aligned on a polypropylene rod seven times to fabricate a seven-layer seamless tube. (C) An oriented collagen tube (OCT). (D) The scanning electron microscopy image of the OCT indicating the orientation of collagen fibers. Scale bar = 10 μm.

consecutive fashion, which is either ascending or descending. In the absence of a paw withdrawal response to the selected force, a stronger stimulus was applied. In the presence of paw withdrawal as a positive response, a weaker stimulus was chosen. In accordance a previous study [31], after the response threshold was first crossed (the two responses straddling the threshold), four additional stimuli were applied. On the basis of responses to the series of stimuli applied using the Von Frey filament, the 50% paw withdrawal threshold was calculated.

2.4. Histological analysis

The OCT implants were harvested from the resected area 2 and 4 weeks after implantation and fixed in 4% paraformaldehyde in phosphate buffered saline (PBS). Following fixation, the tissues were embedded in paraffin, sliced to obtain longitudinal and transverse sections of 5 μm thickness, and stained with hematoxylin and eosin (H&E). The extent of tissue regeneration was analyzed by measuring the maximum diameter at the central region in the regenerated tissue by using the longitudinal sections. Five sections were randomly chosen and used to collect data for comparison between 2-week and 4-week time points after surgery.

Overnight staining with Luxol Fast Blue (LFB) dye was performed at 56 °C to visualize the myelin sheath in the resected area. LFB-positive areas were measured using Image-J software (National Institutes of Health, Bethesda, MD, USA) in a standardized field (320 μm × 240 μm) on the proximal, central, and distal regions in the intact group and OCT group. A total of 15 sites (five slides/group) were randomly selected from each specimen corresponding to the 2-week and 4-week timepoints after surgery.

2.5. Immunohistochemical analysis

Regenerated tissues were subjected to immunohistochemical analysis to determine the extent of myelination. After paraffin-embedded sections (5-μm thick) were prepared, rabbit polyclonal

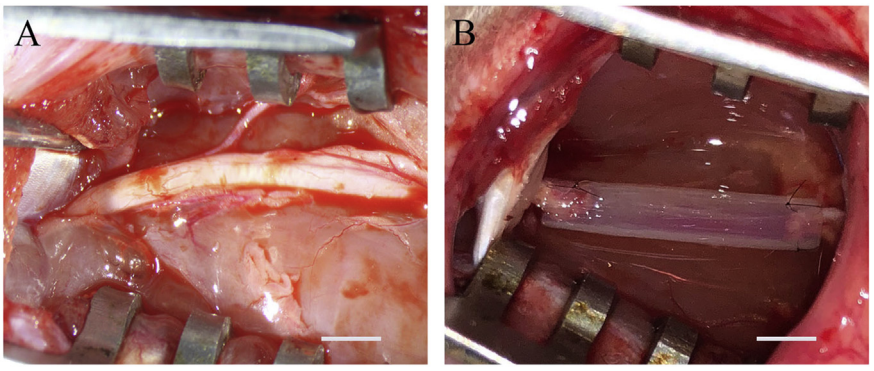

Fig. 2. OCT implantation. (A) After dissecting the skin of the left thigh, the left sciatic nerve is exposed. (B) A 10-mm long portion of the left sciatic nerve is resected. The OCT is indwelled, and the nerve stump and the OCT are suture at 2 places each with 10-0 nylon thread. Scale bar = 3 mm.

anti-myelin basic protein (MBP) antibodies (ab40390, 1:500; Abcam, Cambridge, UK) were used to label the myelin sheath, rabbit polyclonal anti S100B antibodies (701340, 1:50; Thermo Fisher, Waltham, MA, USA) were observed the distribution of Schwann cells, and rabbit monoclonal anti-CD34 antibodies (ab 81289, 1: 100; Abcam) were observed the distribution of endothelial cells. The sections were treated with the antibodies overnight at 4 °C after blocking the endogenous peroxidase activity with 3% hydrogen peroxide in methanol for 20 min at 22 ± 3 °C and antigen retrieval in HistoVT One (Nacalai Tesque, Kyoto, Japan) for 20 min at 90 °C. ImmPRESS horseradish peroxidase anti-rabbit or anti-mouse IgG (peroxidase) polymer detection kit (Vector Laboratories, Burlingame, Ca., USA) was then applied for 30 min (22 ± 3 °C). Sections were incubated with diaminobenzidine substrate (Vector Laboratories) to visualize immunoreactivity.

Areas of the MBP-positive and S100B-positive regions in the field of 320 × 240 μm (5 slides/group) at a high magnification (40×) were measured at the proximal, central, and distal region using Image-J software (National Institutes of Health) respectively. To compare the number of blood vessels in the regenerated nerve tissue, total number of blood vessels with the presence of CD34-positive cells within one nerve tissue was counted in one transverse sectional image of the central region of the nerve tissues per group (OCT and intact groups). The average number of blood vessels at 2 weeks was compared with the average at 4 weeks after surgery and average at the intact group (n = 5 slides each). To compare the inner diameter of each blood vessel per group (OCT and intact groups), the inner diameter of blood vessels with the presence of CD34-positive cells was measured in the shape of a precise circle excluding blood vessels with oval shapes which were measured using Image-J software. The average inner diameter obtained in fifteen blood vessels from five sections per group was compared between 2-week and 4-week time points after surgery and between the OCT group and the intact group.

2.6. Transmission electron microscopy

After gently removing the OCT, the regenerated nerves excised from rats were fixed in a mixture of 2.5% glutaraldehyde and 2% paraformaldehyde dissolved in PBS for 1 h. After postfixing with 1% osmium tetroxide in PBS for 1 h, the samples were dehydrated in a gradient concentration of ethanol ranging from 50% to 100% and then infiltrated and embedded in pure LR White (medium grade, London Resin Co., Ltd., Berkshire, England). Ultrathin sections of the regenerated nerve at the central region were counterstained with uranyl acetate and lead citrate. Transmission electron microscopy (TEM) images were taken using JEM-1400 Plus system (JEOL Ltd.) to measure the myelin sheath thickness (μm). Ten TEM images were selected from the central region of the regenerated myelin sheath in the OCT group and intact group, and the myelin sheath thickness was calculated from the defined field (35 μm × 26 μm) of the cross section; their average values were compared.

2.7. Statistical analysis

Data are shown as mean ± standard deviation (SD). The significance of differences between groups were determined by using Ekuseru-Toukei software (Version 1.04; Social Survey Research Information Co., Ltd., Tokyo, Japan). The significance of differences in

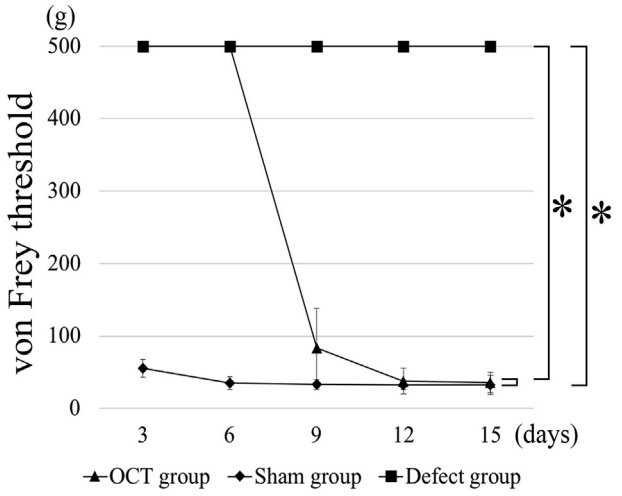

Fig. 3. Von Frey test. Von Frey test performs every 3 days after surgery. There are significant differences between the sham group and the defect group and between the OCT group and the defect group at postoperative day 15 ($P < 0.01$).

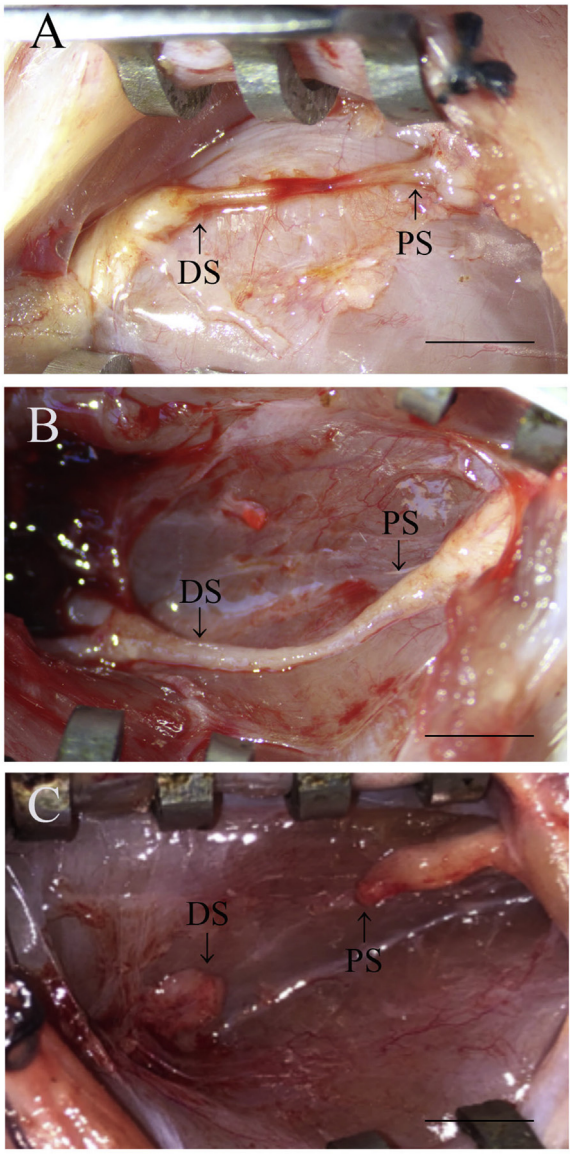

Fig. 4. Gross observation. (A) Image of the sciatic nerve 2 weeks after OCT implantation. (B) Image of the sciatic nerve 4 weeks after OCT implantation. (C) Image of the sciatic nerve in the defect group. PS: Proximal stump; DS: Distal stump. Scale bars = 5 mm.

the thickness of the central region of a nerve, as determined after H&E staining between the 2-week and 4-week time points after OCT implantation were evaluated by Student's t test. One-way analysis of variance with Tukey's test was used to analyze the results of Von Frey test in each group on POD 15, to investigate differences between the OCT implanted side and intact side as determined by LFB staining and immunohistochemical analysis, and to investigate differences in myelin-sheath thickness between OCT implanted and intact sides as determined by electron microscopic image analysis. A P value of <0.05 was considered statistically significant.

3. Results

3.1. Sensory function determined by Von Frey test

Von Frey test showed significant differences among the groups (Fig. 3). The sensory reflexes in the OCT group were restored as well as those in the sham group on POD 15. In the defect group, no recovery of perception could be observed on POD 15.

3.2. Gross appearance of the repaired sciatic nerve

All the surgical procedures were performed well, and the rats survived without any postoperative complications. Because the grafted OCT was not completely absorbed 2 and 4 weeks after implantation, they were gently removed from the grafted site and the regenerated tissues were observed. The 10-mm gap at the injury site was re-bridged and continuous regeneration occurred for 2 weeks after implantation (Fig. 4A). The continuously regenerated tissue was thicker at the 4-week time point than at the 2-week time point (Fig. 4B). Thickness of the regenerated tissue decreased gradually from the proximal and distal stump sides to the central region after 2 weeks. Interestingly, the regenerated tissue at the central region showed congestion; however, the congested region disappeared 4 weeks after implantation. In the defect group, the connective tissue observed in the resected nerve region and the proximal stump did not connect with the distal stump 4 weeks after the surgery (Fig. 4C).

3.3. Morphological analysis of nerve regeneration at the injury site of rat sciatic nerve

Because the proximal stump appeared to be connected with the distal stump on gross observation, the tissue organization in the repair region was analyzed by using H&E staining in the longitudinal section. There was no visible inflammation in the regenerated tissues. Histological analysis revealed crosslinking of the regenerated tissue 2 weeks after surgery (Fig. 5A). Thickness of the regenerated tissues appeared to be higher at the 4-week time point than at the 2-week time point (Fig. 5B). Thickness of the regenerated tissue at the central region was significantly higher at the 4-week time point than at the 2-week time point (Fig. 10A). At a high magnification, the regenerated tissues showed a more organized myelin sheath arrangement in the OCT group at the 4-week time point than at the 2-week time point (Fig. 5C). Notably, because the regenerated myelin sheath on the proximal side appeared similar to that on the intact nerve, remyelination was

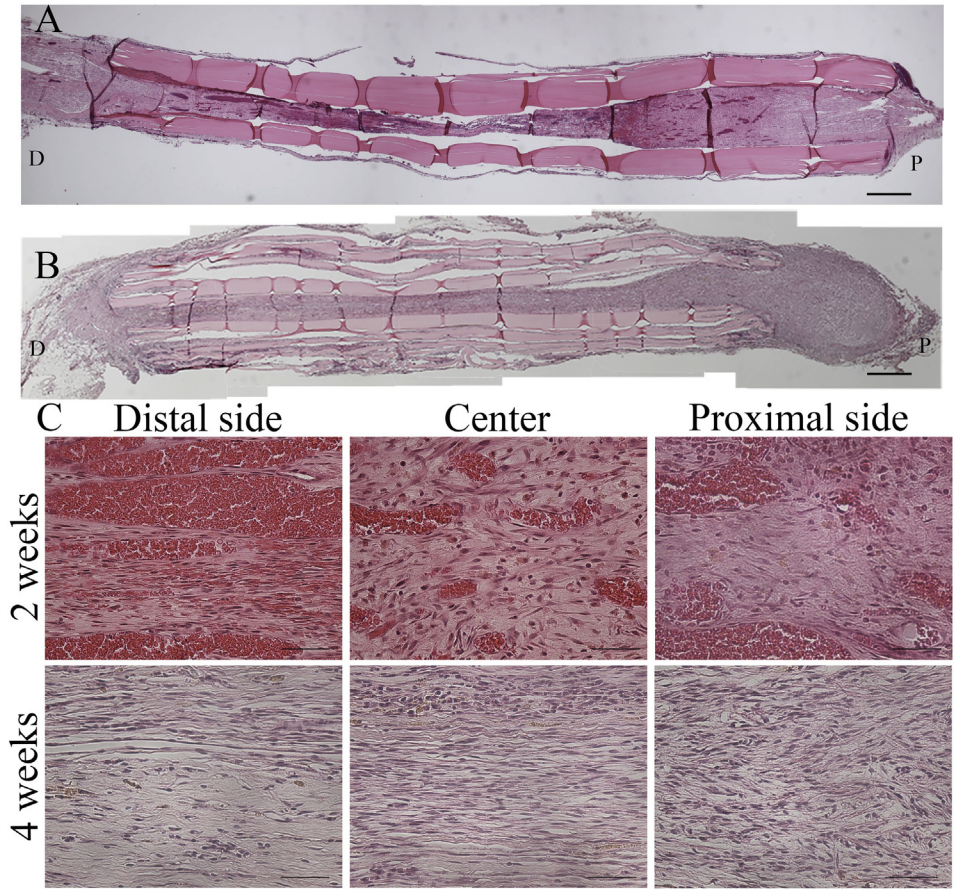

Fig. 5. Histological analysis by H&E staining in the OCT group. (A) Longitudinal image of the regenerated tissues 2 weeks after OCT implantation (B) and 4 weeks after OCT implantation. (C) High-magnification H&E-stained longitudinal images 2 and 4 weeks after surgery. P: Proximal; D: Distal. A, B Scale bars = 500 μm. C Scale bars = 50 μm.

evaluated on the proximal side, central region, and distal side of the repaired site by using anti-MBP antibodies and LFB and S100B stains. LFB staining showed a regularly arranged myelin sheath in the intact group and an irregularly arranged myelin sheath on the proximal side, which completely disappeared from the central region and distal region, in the OCT group after 2 weeks (Fig. 6). Because LFB-positive area was observed on each site, the total myelin sheath area was measured 2 and 4 weeks after the surgery in the OCT group and the intact group by using LFB staining. The magnitude of LFB-positive area tended to differ greatly among the proximal, central, and distal regions in the OCT group 2 and 4 weeks after surgery. In fact, the LFB-positive area was larger in all the regions at the 4-week time point than at the 2-week time point (Fig. 10B).

Fiber sprouting was quantified by measuring the MBP-positive area in each longitudinal section subjected to OCT implantation (Fig. 7). MBP was expressed to some extent in proximal region at the 2-week time point and in all sites at the 4-week time point. The proximal region showed the highest myelin sheath recovery, while the distal side showed a sparse MBP-positive area 2 and 4 weeks after surgery in the OCT group. In addition, there was a significant difference in the total area of the myelin sheath regenerated in all the areas between the 2-week and 4-week time points (Fig. 10C).

S100B staining was used to assess the proliferation of Schwann cells (Fig. 8). There was no significant difference in the S100B-positive area in the proximal region between the 2-week and 4-week time points. On the contrary, the S100B-positive areas in the central region and the distal region were significantly higher after 4 weeks than after 2 weeks post-surgery. Interestingly, there was no significant difference in the S100B-positive area between the proximal and central regions after 4 weeks (Fig. 10D).

Finally, the thickness of regenerated myelin sheath was measured at the central region by using TEM; however, no myelin sheath was observed around the regenerated axons at the central region 2 weeks after surgery in the OCT group (Fig. 9A). The average thickness was 0.423 ± 0.107 μm in the OCT group and 2.151 ± 0.477 μm in the intact group, 4 weeks after surgery (Fig. 9B and C). There was a significant difference in the thickness between the 2-week and 4-week time points in the OCT group (Fig. 9D). However, the myelin thickness of regenerating fibers was significantly lower than the normal thickness.

3.4. Blood vessel analysis

Because the regenerated tissue at the central region showed a congestion on gross observation, the extent of blood vessel formation was evaluated at the central region from the transverse section after 2 weeks and 4 weeks (Fig. 11A, C, E). A large number of blood vessels were observed in the central region after 2 weeks. Angiogenesis is a well-coordinated process involving endothelial cell proliferation, migration, and differentiation. Subsequently, anti-CD34 antibodies were used to detect endothelial cells (Fig. 11B, D, F). The number of blood vessels after 4 weeks was dramatically lower than that after 2 weeks (Fig. 11G). Specifically, the number of blood vessel at the 2-week time point was significantly larger than that at the 4-week time point. In addition, there was no significant difference in the inner diameter of the newly formed blood vessels between the 2-week and 4-week time points in the OCT group (Fig. 11H). However, the inner diameter of newly formed blood vessels in the OCT group was significantly thicker than the normal thickness.

4. Discussion

In this study, OCTs were produced to serve as physical bridges to lesions between the proximal and distal stumps of disconnected nerves. Von Frey test results were almost identical in the OCT group and the sham group on POD 15. Interestingly, the test showed that

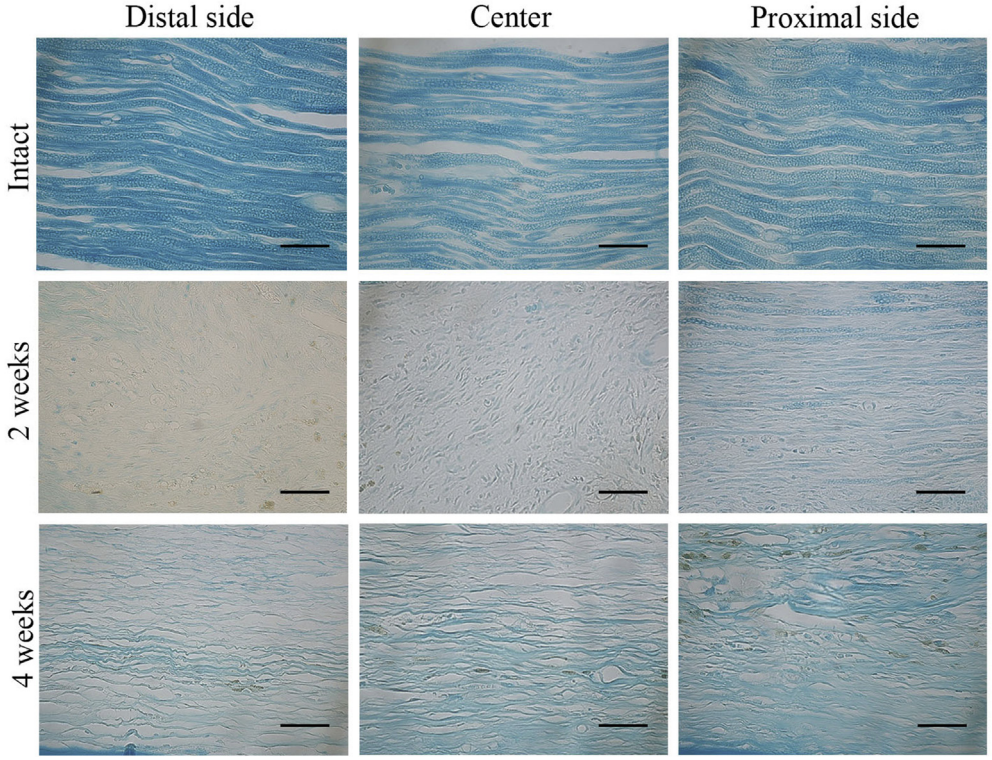

Fig. 6. Histological analysis by using Luxol fast blue (LFB) staining. The longitudinal sections showing the proximal region, central region, and distal region of the regenerated tissue from the intact group and the OCT group (2 weeks and 4 weeks after implantation). Scale bars = 50 μm.

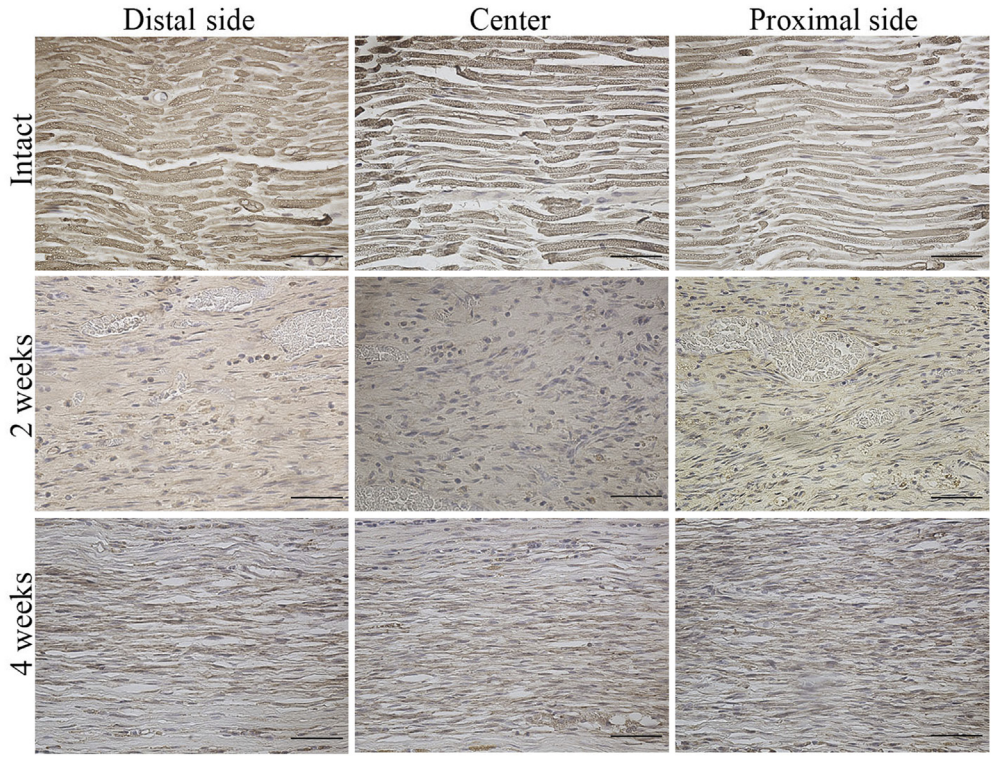

Fig. 7. Myelin basic protein (MBP) expression in the regenerated peripheral nerve. Longitudinal section showing the proximal, central, and distal regions of the regenerated tissue from the intact group and the OCT group (2 weeks and 4 weeks after implantation). Scale bars = 50 μm.

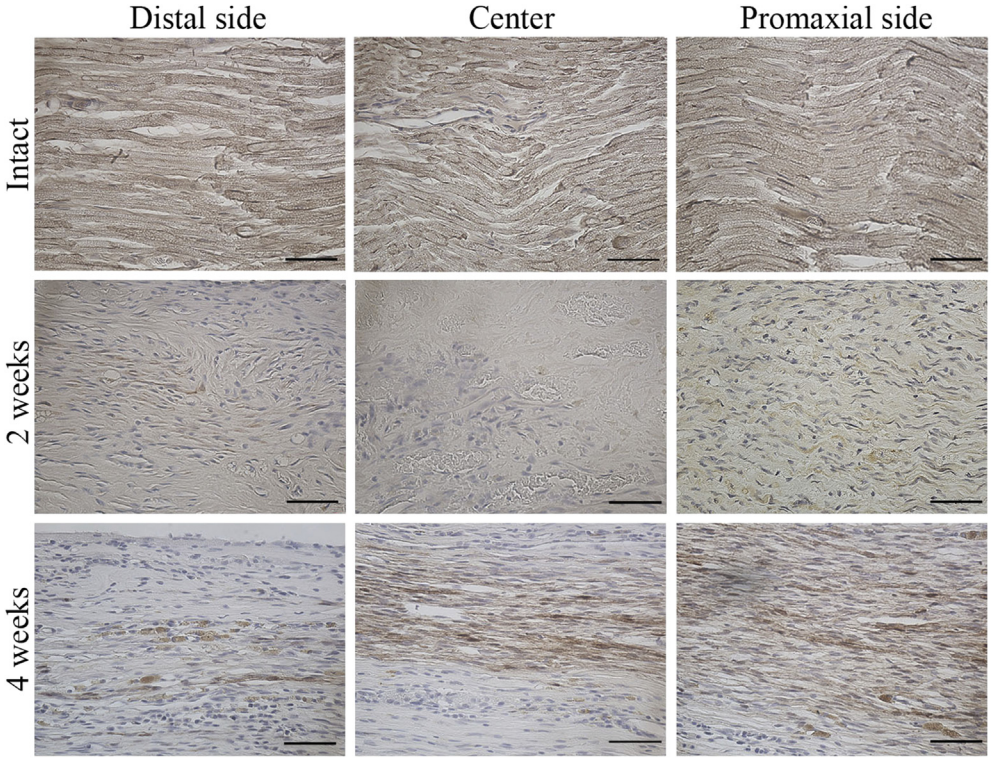

Fig. 8. S100B protein expression in the regenerated peripheral nerve. Longitudinal sections showing the proximal, central, and distal regions of the regenerated tissue from the intact group and the OCT group (2 weeks and 4 weeks after implantation). Scale bars = 50 μm.

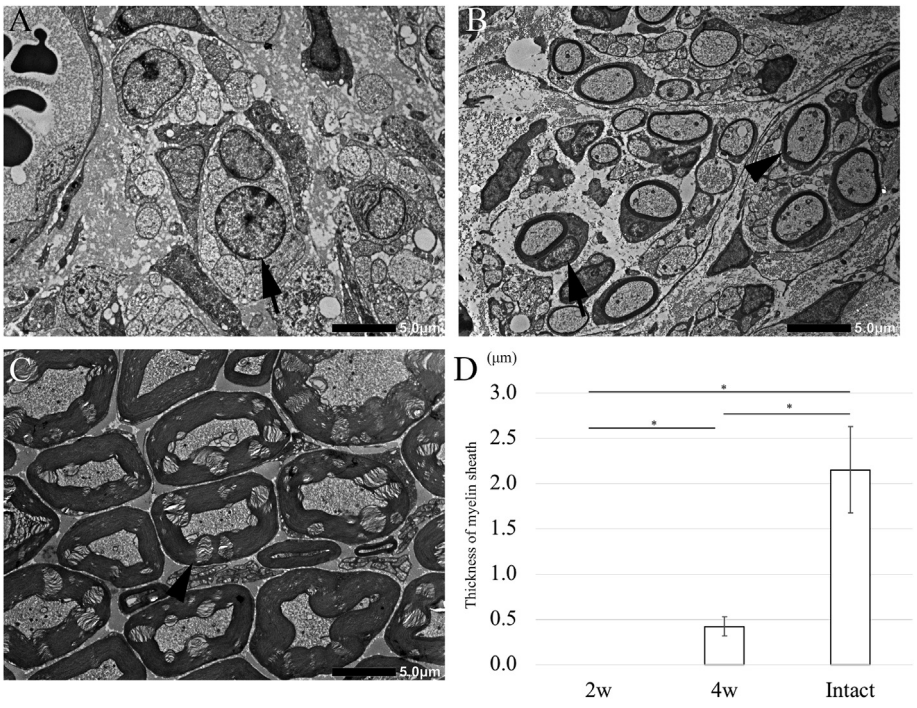

Fig. 9. Transmission electron microscopy images of cross-sections of a regenerated peripheral nerve. (A) 2 weeks after OCT implantation, the nuclei of Schwann cells surround by unmyelinated axons are observed (arrow). (B) 4 weeks after OCT implantation, myelinated axons are observed (arrowhead). (C) Images of intact tissue. (D) The thickness of the myelin sheath as measured using Image-J soft. Ten myelin sheaths are selected from the central region of the regenerated peripheral nerve. The thickness in the OCT group is significantly lower than that in the intact group ($P < 0.01$).

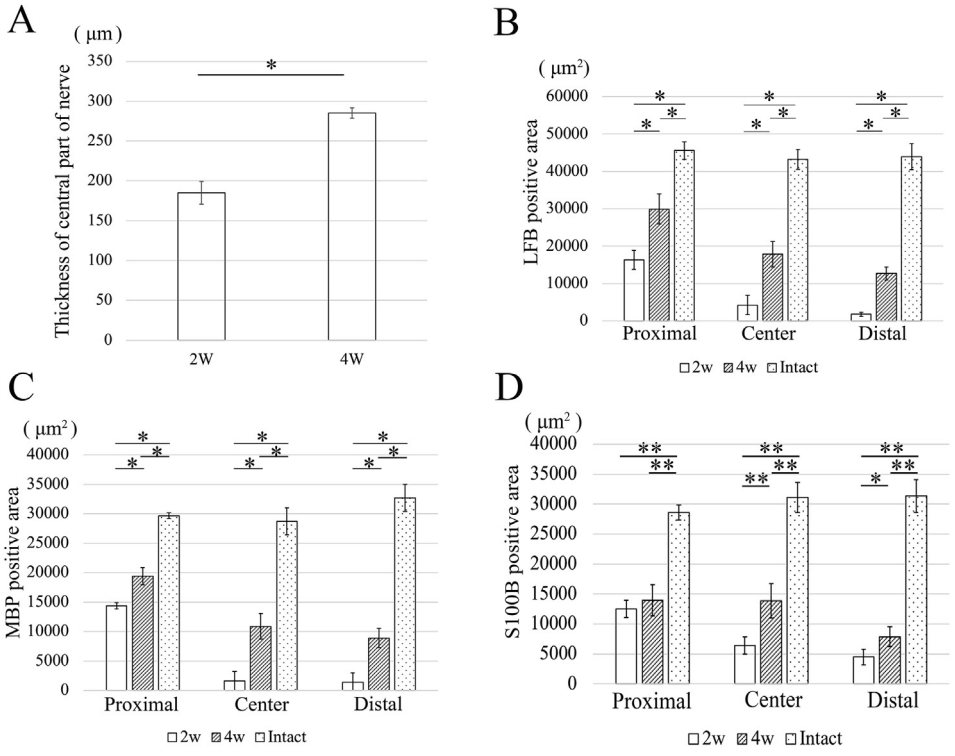

Fig. 10. Results of statistical analyses corresponding to Fig. 5, Fig. 6, Fig. 7, and Fig. 8. (A) The thickness of regenerated tissue at the central region at the 4-week time point is significantly higher than that at the 2-week time point ($P < 0.01$). (B) At the 4-week time point, the LFB-positive area from the proximal to distal region is smaller in the OCT group than that in the intact tissues ($P < 0.01$). (C) At the 4-week time point, the MBP-positive area in the proximal and distal region is smaller than that of the intact tissues. ($P < 0.01$) (D) The S100B positive area in the proximal and the distal regions is smaller than that in the intact tissue at the 4-week time point ($^{*}P < 0.05$; $^{**}P < 0.01$).

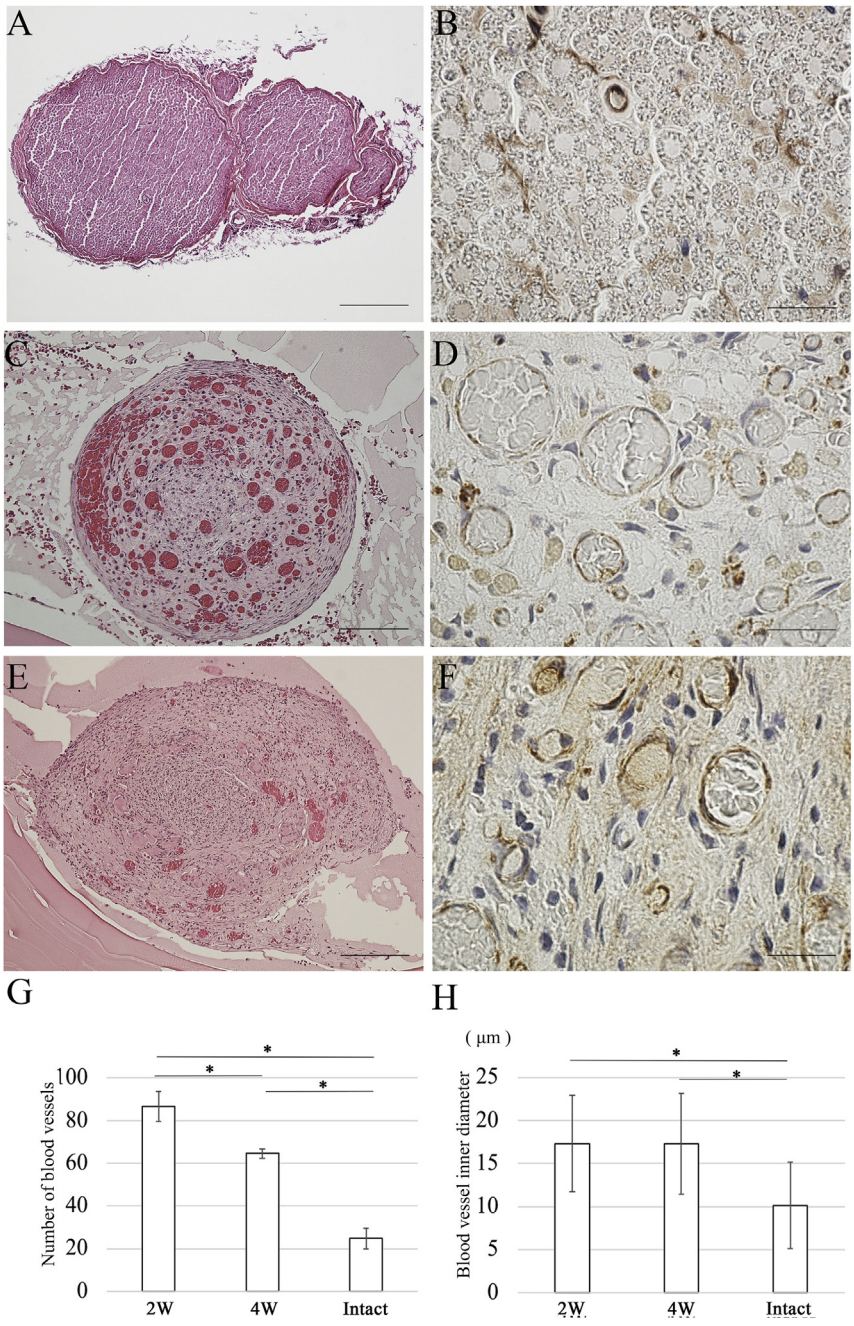

Fig. 11. Evaluation of angiogenesis. Sections of the central region of the regenerated tissues are subjected to H&E staining and immunostaining using anti-CD34 antibodies to detect endothelial cells in the regenerated peripheral nerve. (A) H&E staining image of central region of the regenerated tissue in intact group. (B) Immunostaining using anti-CD34 antibodies: image of the central region of the regenerated tissue in the intact group. (C) H&E staining: image of central region of the regenerated tissue 2 weeks after OCT implantation. (D) Immunostaining using anti-CD34 antibodies: image of the central region of the regenerated tissue 2 weeks after OCT implantation. (E) H&E staining: image of the central region of the regenerated tissue 4 weeks after OCT implantation. (F) Immunostaining using anti-CD34 antibodies: image of the central region of the regenerated tissue 4 weeks after OCT implantation. (G) The number of blood vessels is higher in the OCT group than in the intact group ($P < 0.01$). (H) The inner diameter of newly formed blood vessels in the OCT group is significantly thicker than the normal thickness ($P < 0.01$). A, E Scale bars = 200 μm. C Scale bars = 100 μm. B, D, F Scale bars = 20 μm.

the sensory function recovered dramatically from POD 6 to POD 9. Subsequently, the recovery of the transected sciatic nerve was observed by gross observation because the primary nerve repair requires a direct approximation of the proximal and distal stumps. The proximal stump was observed to be connected with the distal stump on POD 7 (data not shown). In addition, the thickness of the regenerated bridges inside the OCT increased gradually until 4 weeks after surgery. These results suggest that there may be a correlation between the sensory function and the tissue connection. Subsequently, we examined the histological recovery of the regenerated tissues by using H&E staining. Staining the longitudinal sections clearly confirmed that newly regenerated tissues connected the proximal and distal stumps. However, there was a difference in the thickness of the regenerated tissues depending on the region from the proximal to distal end. Interestingly, the proportion of the area occupied by the blood vessels in the regenerated tissue was quite different depending on the region, after 2 weeks. In a high magnification image, the proximal region

showed blood vessels around the regenerated tissues. On the contrary, in the distal region, the blood vessels were observed in the center of the regenerated tissues.

Because the connection between the proximal and distal stumps was observed by H&E staining, histological analysis of myelinated axons by LFB and MBP immunohistological staining demonstrated the histological recovery of nerve tissue because, during nerve regeneration, the myelination of nerve fibers was a marker that determines the intensity of nerve regeneration. MBP is a major constituent of the myelin sheath produced by Schwann cells in the peripheral nervous system. The difference between the proximal and distal regions observed by LFB staining was consistent with that observed by MBP staining. After 2 weeks, myelin sheaths were detected in the proximal region but not in the central and distal regions. The myelin sheath was observed in the central and distal regions after 4 weeks. The results suggested that distances of penetration from the proximal nerve stump are shown by LFB/MBP staining. In addition, the patterns of LFB/MBP staining were remarkably similar to that of S100B staining, which helps detect Schwann cells. Because there were clear histological differences in tissue regeneration between the 2-week and 4-week time points depending on the region, the LFB-/MBP-/S100B-positive areas were measured. LFB/MBP/S100B positivity at the 4-week time point was clearly higher than that at the 2-week time point. The results suggested that both regenerated axons and Schwann cells existed and facilitated the process of myelination and that of the structural recovery of regenerated nerve tissues. In addition, the results are mainly attributed to the following reasons. OCTs provide adequate space for the adhesion of the Schwann cells and promote the regeneration of myelin sheaths along the rectilinear direction inside the OCTs.

However, the areas of the myelin sheaths determined by LFB/MBP/S100B staining in the OCT group were significantly lower than that in the intact group at the 4-week time point. Therefore, myelination of the regenerated nerve tissues was further examined by TEM analysis. Complete myelination was not observed at the 2-week time point in the central region, a finding that is consistent with that of our immunohistological analysis. On the contrary, although myelination was observed at the 4-week time point, the thickness of myelin sheath in the OCT group was significantly lower than that in the intact group. Peripheral nerves consist of bundles of axons, and each axon is associated with and enveloped by Schwann cells, which myelinate them. In contrast, peripheral nerves consist of smaller grouped unmyelinated axons in structures known as Remark bundles [18,19,33,34]. In summary, when the sensory function was normally recovery on POD 15, the regenerated nerve-tissue bridge was mainly composed of unmyelinated axons.

Many studies have revealed that increasing angiogenesis within conduits enhances axonal growth, resulting in a better nerve recovery [35]. Another study described that blood vessels are necessary and sufficient to guide the migration of Schwann cells [36]. As mentioned above, the regenerated nerve tissues are sufficiently vascularized within the OCT to allow a meaningful quantification of CD34-positive area using CD34 as the endothelial cell marker. The regenerated nerve tissues showed a larger number of blood vessels at the 2-week time point than at the 4-week time point and in the intact tissue in this study. In summary, OCT provides a more conductive environment for the migration of endothelial cells to form new blood vessels. Unfortunately, because direct functional assessment in a rat is difficult, the authors stress that the aim of the current investigation was to perform a histological analysis using anti-CD34 immunohistochemical staining. This may be considered a limitation of our study.

Furthermore, a previous study suggested that the vascular response to crush and transection injury is composed to two phases [37]. The early phase comprises the first week after injury, and it is characterized by an increase in blood vessel size, but not the blood vessel number. During the second phase, 1–6 weeks after injury, an increase in the number of vessels is observed. The number of blood vessels and their inner diameter were measured in this study. Our results are consistent with those of a previous report on vascular regrowth [37]. These results indicated the effect of OCT on sciatic nerve regeneration by demonstrating a positive relationship between increased vascularization and enhanced nerve regeneration. Another previous study suggested the importance of microvessels in guiding nerve regeneration and supporting neuronal survival [38]. Our results also showed that a difference in the area of regenerated myelin sheath between the proximal and the distal region indicates that vascularization may be a priority before the reinnervation of the myelin sheathe. However, the link between vascular guidance and the effect of OCT was not examined in this study.

5. Conclusion

In conclusion, the OCTs guide the growth of myelin sheath from the nerve stumps for the recovery of sensory function in the peripheral nervous system. In addition, OCTs provide an optimal microenvironment for vascularization during the repair of a transected sciatic nerve. The oriented collagen fiber in the OCT may influence the growth of the endothelial cells. In the future, nerve regeneration may be enhanced by manipulating vascularization.

Declaration of Competing Interest

The authors declare no conflict of interest.

Acknowledgements

This work was supported by JSPS KAKENHI Grant Numbers JP17K11925, JP16K11703.

References

[1] Faroni A, Mobasseri SA, Kingham PJ, Reid AJ. Peripheral nerve regeneration: experimental strategies and future perspectives. Adv Drug Deliv Rev 2015;82–83:160–7.
[2] Raso VV, Barbieri CH, Mazzer N, Fasan VS. Can therapeutic ultrasound influence the regeneration of peripheral nerves? J Neurosci Methods 2005;142(2):185–92.
[3] Matsuyama T, Mackay M, Midha R. Peripheral nerve repair and grafting techniques: a review. Neurol Med Chir (Tokyo) 2000;40(4):187–99.
[4] Jiang B, Zhang P, Zhang D, Fu Z, Yin X, Zhang H. Study on small gap sleeve bridging peripheral nerve injury. Artif Cells Blood Substit Immobil Biotechnol 2006;34(1):55–74.
[5] Oprych KM, Whitby RL, Mikhalovsky SV, Tomlins P, Adu J. Repairing peripheral nerves: is there a role for carbon nanotubes. Adv Healthc Mater 2016;5(11):1253–71.
[6] Isobe Y, Kosaka T, Kuwahara G, Mikami H, Saku T, Kodama S. Oriented collagen scaffolds for tissue engineering. Materials (Basel) 2012;5(3):501–11.
[7] Sosa I, Reyes O, Kuffler DP. Immunosuppressants: neuroprotection and promoting neurological recovery following peripheral nerve and spinal cord lesions. Exp Neurol 2005;195(1):7–15.
[8] Yang Y, Yuan X, Ding F, Yao D, Gu Y, Liu J, et al. Repair of rat sciatic nerve gap by a silk fibroin-based scaffold added with bone marrow mesenchymal stem cells. Tissue Eng A 2011;17(17–18):2231–44.
[9] Doolabh VB, Hertl MC, Mackinnon SE. The role of conduits in nerve repair: a review. Rev Neurosci 1996;7(1):47–84.
[10] Weiss P. Experiments on cell and axon orientation in vitro; the role of colloidal exudates in tissue organization. J Exp Zool 1945;100:353–86.
[11] Ceballos D, Navarro X, Dubey N, Wendelschafer-Crabb G, Kennedy WR, Tranquillo RT. Magnetically aligned collagen gel filling a collagen nerve guide improves peripheral nerve regeneration. Exp Neurol 1999;158(2):290–300.
[12] Dubey N, Letourneau PC, Tranquillo RT. Guided neurite elongation and schwann cell invasion into magnetically aligned collagen in simulated peripheral nerve regeneration. Exp Neurol 1999;158(2):338–50.

[13] Guido S, Tranquillo RT. A methodology for the systematic and quantitative study of cell contact guidance in oriented collagen gels. Correlation of fibroblast orientation and gel birefringence. J Cell Sci 1993;105(Pt 2):317–31.
[14] Matsugaki A, Isobe Y, Saku T, Nakano T. Quantitative regulation of bone-mimetic, oriented collagen/apatite matrix structure depends on the degree of osteoblast alignment on oriented collagen substrates. J Biomed Mater Res A 2015;103(2):489–99.
[15] Fawcett JW, Keynes RJ. Peripheral nerve regeneration. Annu Rev Neurosci 1990;13:43–60.
[16] Torigoe K, Tanaka HF, Takahashi A, Awaya A, Hashimoto K. Basic behavior of migratory Schwann cells in peripheral nerve regeneration. Exp Neurol 1996;137(2):301–8.
[17] Hall S. Nerve repair: a neurobiologist's view. J Hand Surg Br 2001;26(2):129–36.
[18] Bunge RP. The role of the Schwann cell in trophic support and regeneration. J Neurol 1994;242(1 Suppl 1):S19–21.
[19] Guenard V, Kleitman N, Morrissey TK, Bunge RP, Aebischer P. Syngeneic Schwann cells derived from adult nerves seeded in semipermeable guidance channels enhance peripheral nerve regeneration. J Neurosci 1992;12(9):3310–20.
[20] Holmes W, Young JZ. Nerve regeneration after immediate and delayed suture. J Anat 1942;77(Pt 1):63–96. 10.
[21] Ide C, Tohyama K, Yokota R, Nitatori T, Onodera S. Schwann cell basal lamina and nerve regeneration. Brain Res 1983;288(1–2):61–75.
[22] Scherer SS, Easter Jr SS. Degenerative and regenerative changes in the trochlear nerve of goldfish. J Neurocytol 1984;13(4):519–65.
[23] Thompson DM, Buettner HM. Neurite outgrowth is directed by schwann cell alignment in the absence of other guidance cues. Ann Biomed Eng 2006;34(1):161–8.
[24] Zhang H, Gally C, Labouesse M. Tissue morphogenesis: how multiple cells cooperate to generate a tissue. Curr Opin Cell Biol 2010;22(5):575–82.
[25] Eaton S, Julicher F. Cell flow and tissue polarity patterns. Curr Opin Genet Dev 2011;21(6):747–52.
[26] Thery M, Racine V, Piel M, Pepin A, Dimitrov A, Chen Y, et al. Anisotropy of cell adhesive microenvironment governs cell internal organization and orientation of polarity. Proc Natl Acad Sci U S A 2006;103(52):19771–6.
[27] Matsugaki A, Fujiwara N, Nakano T. Continuous cyclic stretch induces osteoblast alignment and formation of anisotropic collagen fiber matrix. Acta Biomater 2013;9(7):7227–35.
[28] Fujimaki H, Uchida K, Inoue G, Miyagi M, Nemoto N, Saku T, et al. Oriented collagen tubes combined with basic fibroblast growth factor promote peripheral nerve regeneration in a 15 mm sciatic nerve defect rat model. J Biomed Mater Res A 2017;105(1):8–14.
[29] Rustemeyer J, Gregersen J. Quality of Life in orthognathic surgery patients: post-surgical improvements in aesthetics and self-confidence. J Craniomaxillofac Surg 2012;40(5):400–4.
[30] Hillerup S. Iatrogenic injury to the inferior alveolar nerve: etiology, signs and symptoms, and observations on recovery. Int J Oral Maxillofac Surg 2008;37(8):704–9.
[31] Chaplan SR, Bach FW, Pogrel JW, Chung JM, Yaksh TL. Quantitative assessment of tactile allodynia in the rat paw. J Neurosci Methods 1994;53(1):55–63.
[32] Dixon WJ. Efficient analysis of experimental observations. Annu Rev Pharmacol Toxicol 1980;20:441–62.
[33] Fraher J, Dockery P. A strong myelin thickness-axon size correlation emerges in developing nerves despite independent growth of both parameters. J Anat 1998;193(Pt 2):195–201.
[34] Chen YY, McDonald D, Cheng C, Magnowski B, Durand J, Zochodne DW. Axon and Schwann cell partnership during nerve regrowth. J Neuropathol Exp Neurol 2005;64(7):613–22.
[35] Kakihata CM, Malanotte JA, Karvat J, Brancalhão RM, de Fátima Chasko Ribeiro L, Bertolini GR. The morphological and functional effects of exercise in the aquatic environment, performed before and/or after sciatic nerve compression in Wistar rats. J Exerc Rehabil 2016;12(5):393–400.
[36] Cattin AL, Burden JJ, Van Emmenis L, Mackenzie FE, Hoving JJ, Garcia Calavia N, et al. Macrophage-induced blood vessels guide schwann cell-mediated regeneration of peripheral nerves. Cell 2015;162(5):1127–39.
[37] Hobson MI, Brown R, Green CJ, Terenghi G. Inter-relationships between angiogenesis and nerve regeneration: a histochemical study. Br J Plast Surg 1997;50(2):125–31.
[38] Bearden SE, Segal SS. Microvessels promote motor nerve survival and regeneration through local VEGF release following ectopic reattachment. Microcirculation 2004;11(8):633–44.